Food Chemistry: X 17 (2023) 100533

Contents lists available at ScienceDirect

Food Chemistry: X

journal homepage: www.sciencedirect.com/journal/food-chemistry-x

A comparison study on polysaccharides extracted from *Rosa sterilis* S.D.Shi using different methods: Structural and *in vitro* fermentation characterizations

Shiguo Chen [a,b,c,d,e,f,1], Luqin Luan [a,1], Yanru Zhang [a], Feifei Liu [a], Xingqian Ye [a,b,c,d,e,f], Zhiqiang Hou [a,*]

[a] College of Biosystems Engineering and Food Science, National-Local Joint Engineering Laboratory of Intelligent Food Technology and Equipment, Zhejiang Key Laboratory for Agro-Food Processing, Zhejiang Engineering Laboratory of Food Technology and Equipment, Zhejiang University, Hangzhou 310058, China
[b] Zhejiang University Zhongyuan Institute, Zhengzhou 450000, China
[c] Innovation Center of Yangtze River Delta, Zhejiang University, Jiaxing 314102, China
[d] Shandong (Linyi) Institute of Modern Agriculture, Zhejiang University, Linli 276000, China
[e] Fuli Institute of Food Science, Zhejiang University, Hangzhou 310058, China
[f] Ningbo Research Institute, Zhejiang University, Hangzhou 315100, China

ARTICLE INFO

Keywords:
Rosa sterilis
Polysaccharides
Extraction methods
Structure
Gut microbiota

ABSTRACT

In this study, the structural and *in vitro* fermentation characterizations of *Rosa sterilis* S.D.Shi polysaccharides (RSP), extracted by hot water (HW), acid (AA), alkali (AK) and enzyme (EM) were investigated for the first time. The results indicated that extraction methods exhibited significant effects on the structure of RSPs, thus resulting in different probiotic effects. HW-RSP and AA-RSP had high contents of Gal, Glc and GalA, while AK-RSP and EM-RSP mainly contained Ara, Gal and GalA. EM-RSP was rich in RG-I and its size of average side chain were the largest. Moreover, HW-RSP and AK-RSP exhibited the smallest (57.55 kDa) and largest (922.20 kDa) molecular weights, respectively. All RSPs promoted the production of total SCFAs and the growth of beneficial bacteria like *Bifidobacterium*, *Bacteroides, Faecalibacterium* and *Paraclostrium* to varying degrees, but inhibited the growth of pathogenic bacteria such as *Escherichia-shigella*, thereby regulating the composition of gut microbiota. Furthermore, the function prediction results showed that EM-RSP had the most special metabolic pathways. Collectively, our findings provide new insights into the relationship between the structure and probiotic function of RSPs, and offer theoretical basis for the development of functional products of *Rosa sterilis* S.D.Shi.

Introduction

R. sterilis S.D.Shi., which belongs to the family Rosaceae, is a newly endemic variety discovered by Guizhou Botanical Garden more than 30 years ago (Hou et al., 2020). *R. sterilis* S.D.Shi has a close genetic relationship to *Rosa roxburghii* Tratt., mainly growing in the altitudes varying between 1000 and 1600 m in hilly mountain areas, is an important wild resource in the provinces of southwest, central-south and northwest China (Chen & Kan, 2018). Most studies focused on the chemical components and biological activities of *R. roxburghii* Tratt., indicating that it is rich in ascorbic acid, polysaccharide, phenolics and superoxide dismutase and has potential to prevent type 2 diabetes, inhibit the growth of cancer cells and fight atherosclerosis (Xu, Vidyarthi, Bai, & Pan, 2019). But the research on *R. sterilis S.D.Shi* is still lacking now, which mainly focused on its fruit traits and nutritional components, such as vitamin C, trace elements, amino acid, flavonoids and triterpenes (Liu, Zhang, Zhang, Lu, Fu, & He, 2016).

The polysaccharides extracted from *R. roxburghii* Tratt. have attracted attention recently due to their biological properties including antioxidant, α-D-glucosidase inhibition, digestion and probiotics (Wang et al., 2018; Wang, Li, Huang, Fu, & Liu, 2019). The main extraction methods of *R. roxburghii* Tratt. polysaccharide mentioned already were hot water extraction (HW, liquid-to-solid ratio, 30:1 (w/w); 95 ℃; 3 h) (Wang, Chen, Zhang, Huang, Fu, & Li, 2018), microwave-assisted enzyme extraction (microwave power, 575 W; microwave time, 18 min; liquid-to-material ratio, 13.5:1 mL/g; and enzyme dose, 6.5 g/mL)

* Corresponding author.
E-mail address: houzhiqiang@zju.edu.cn (Z. Hou).
[1] Authors contributed equally to the work.

https://doi.org/10.1016/j.fochx.2022.100533
Received 27 January 2022; Received in revised form 27 October 2022; Accepted 1 December 2022
Available online 5 December 2022

(Wang et al., 2018) and ultrasonic assisted extraction (liquid-to-material, 402:10 mL/g; ultrasound power, 148 W; 80℃; 30 min) (Chen and Kan, 2018). Besides, some other methods were also used to extract polysaccharides from other plants including acid extraction (AA), alkali extraction (AK) and enzyme extraction (EM) (Huang, Chen, Yang, & Huang, 2021). HW is a traditional method, it is easy to operate but time-consuming; AA or AK is more suitable for some polysaccharides, but the pH should be strictly controlled during extraction; EM could accelerate the extraction of polysaccharides under relatively mild conditions; ultrasonic and microwave assisted extraction can also effectively shorten the extraction time, but their equipment costs are also relatively high. Different extraction methods would cause the difference in the composition and structure of polysaccharides, thus affecting their biological activity (Song et al., 2021; Sun et al., 2018).

In recent years, more and more people have noticed that human gut microbiota are closely related to many problems such as obesity, intestinal inflammation, cardiovascular disease, colorectal cancer and etc. (Gentile & Weir, 2018). The composition of human gut microbiota can be affected by the host diet (Ndeh & Gilbert, 2018). The human gut microbiota can ferment complex polysaccharides in the host diet to produce oligosaccharides, short-chain fatty acids (SCFAs) and other metabolites, which may have some effects on human health (Gentile and Weir, 2018). SCFAs, mainly acetate, propionate and butyrate, can serve as energy substrates for intestinal epithelial cells (Koh, De Vadder, Kovatcheva-Datchary, & Backhed, 2016), reduce intestinal pH to inhibit the growth of harmful pathogens (Huang et al., 2019), and improve intestinal immunity (Ndeh and Gilbert, 2018).

Pectin is an important polysaccharide in plant cell wall and contains three main structural domains: homogalacturonan (HG), rhamnogalacturonan I (RG-I) and rhamnogalacturonan II (RG-II), which can be affected by extraction methods (Zhu et al., 2020). Recent studies have shown that RG-I domain has better intestinal probiotic effect after fermentation by human gut microbiota (Hou et al., 2022; Mao et al., 2019; Zhu et al., 2020). For example, the research reported that highly branched RG-I (70.44 %) in citrus pectin can alleviate obesity induced by a high-fat diet (Zhu et al., 2020). Polysaccharides rich in RG-I domain are therefore considered to be a potential prebiotic (Hou et al., 2022; Mao et al., 2019).

However, to date, there are no studies on *R. sterilis* S.D.Shi polysaccharides (RSP) thus its composition, structure and function are still unknown. Furthermore, little information is available on the association with the extraction methods, characterizations and biological activities. So in this study, four extraction methods including HW, AA, AK and EM were used to extract polysaccharides from *R. sterilis* S.D.Shi and their composition, structure and *in vitro* fermentation characterizations were compared in order to provide new insights into the relationship between the structure and probiotic function of RSPs, and offer theoretical basis for the development of high value-added products.

Materials and methods

Materials

R. sterilis S.D.Shi fruits were purchased from Chungui Health Technology Co., ltd (Guizhou, China) in September 2020. The fruits were washed and dried in a blast drying oven (GZX-9070MBE, Bo Xun Medical Biological Instrument Corp, Shanghai, China) at 50 ℃ for 48 h. Dried fruits were then ground by a grinder and passed through a 60-mesh sieve. Cellulase and papain were purchased from Shanghai Yuanye Biotechnology Co., ltd (Shanghai, China). Monosaccharide standards [$_{D}$-glucose (Glc), $_{D}$-galactose (Gal), $_{D}$-mannose (Man), $_{L}$-rhamnose (Rha), $_{D}$-arabinose (Ara), $_{D}$-Fructose (Fuc), $_{D}$-galacturonic acid (GalA) and $_{D}$-glucuronic acid (GlcA)], SCFAs (acetic acid, propionic acid, butyric acid, isobutyric acid, valeric acid and isovaleric acid), 1-Phenyl-3-methyl-5-pyrazolone (PMP) and Inulin were obtained from Sigma-Aldrich Co., ltd (St. Louis, MO, USA). All the other reagents were of analytical grade.

Extraction of RSPs

Before extracting polysaccharides from previously obtained powder, the powder was refluxed with 95 % ethanol twice at 70 ℃ (DF-101S, Gongyi Yuhua Instruments Co., ltd, Henan, China) for 3 h to remove liposoluble compounds and impurities. The filter residue was obtained by vacuum filtration (RE3000A, Shanghai Yarong biochemical instrument factory, Shanghai, China) and air-dried until there was no ethanol flavor and then used for extraction.

Hot water extraction (HW)

The dry powder (5 g) was extracted with 200 mL of distilled water twice at 80 ℃ for 90 min. After vacuum filtration, the filtrate was concentrated to one-quarter of the original volume by vacuum and reduced pressure at 45 ℃. Afterwards, the concentrated liquid was deproteinized by the trichloroacetic acid (TCA, 5 %, w/v) for several times until there is no precipitation. The purified solution was decolorized by AB-8 macroporous resin (macroporous resin: solution = 1:6), oscillating at 37 ℃ for 8 h. Then the RSP were precipitated from the filtrate by adding twice the volume of dehydrated ethanol and keeping overnight at 4℃. The precipitate was separated by centrifugation at 8000 rpm for 10 min (3 K15, Sigma Laboratory Centrifuges, Osterode, Germany) and then collected, dissolved in distilled water again. After dialyzing with a 10 kDa dialysis bag for 72 h and freeze-drying, the HW-RSP was obtained. The extraction yield (Y) of RSP was calculated using the following equation:

$$Y(\%) = \frac{\text{weight of dried RSP (g)}}{\text{weight of } \textit{R.sterilis S.D.Shi} \text{ fruits podwer (g)}} 100\ \%\ (1)$$

Acid extraction (AA)

The dry powder (5 g) was extracted with 200 mL of distilled water at 85 ℃ for 90 min, using 0.1 M HCl solution to adjust the pH to 2.5. After the extraction, the pH of the mixture was adjusted to 5.0– 6.0 with 3 M NaOH. And then filtrated, the filtrate was concentrated to one-quarter of the original volume by vacuum and reduced pressure at 45 ℃. The following procedures were conducted as described in Section 2.2.1.

Alkali extraction (AK)

The dry powder (5 g) was added into 200 mL of 0.1 M NaOH solution and then the pH of the mixture was adjusted to 13 with 4 M NaOH. After 30 min of reaction at room temperature, the pH of the mixture was adjusted to 5.0–6.0 with 0.1 M HCl. The solid residue was removed by filtration and the filtrate was concentrated to one-quarter of the original volume by vacuum and reduced pressure at 45 ℃. The protein was removed by enzymatic method, which was carried out with 0.2 % papain (2500 U/mg) solution at 50 ℃ for 2 h, and then heated at 100 °C for 10 min. The precipitate was separated by centrifugation at 6000 rpm for 10 min and the supernatant was decolored, precipitated, dialyzed and lyophilized as described in Section 2.2.1.

Enzyme extraction (EM)

The dry powder (5 g) was mixed with 200 mL of distilled water (pH 4.5–6.5). The extraction temperature and time were set as 50 ℃ and 120 min, respectively. Before extraction, 2 % cellulase (50 U/mg) was added to the solution, which was dissolved in distilled water (1:1) at 50 ℃ for 10 min. After heating at 100 °C for 10 min, the mixture was centrifuged at 6000 rpm for 10 min and the supernatant was concentrated, deproteinized, decolored, precipitated, dialyzed and lyophilized as described in Section 2.2.1.

Chemical analysis

The total sugar content was measured by phenol–sulfuric acid method (Dubois, Gilles, Hamilton, Rebers, & Smith, 1951), taking $_{D}$-

glucose as the standard. A standard curve of y = 7.9771x − 0.0325 (R^2 = 0.9977) was used to calculate the total sugar content of RSPs, where y and × are the absorbance (Abs) and the content of D-glucose (μg), respectively. The protein content was measured by Bradford's method (Bradford, 1976), using bovine serum albumin as the standard. The standard curve was y = 0.0069x + 0.0161, R^2 = 0.9951, where y and x are the Abs and the content of bovine serum albumin (μg), respectively.

Monosaccharide composition analysis

Monosaccharide composition of the RSPs were analyzed by HPACE-PAD on an ICS-5000 system (Thermo Fisher, USA) equipped with a CarboPac PA10 column (4 mm × 250 mm, Thermo Fisher, USA) and an electrochemical detector (ECD). Gradient elution was employed, with an isocratic NaOH (18 mM) for 15 min, followed by isocratic sodium acetate (100 mM) containing a fixed 18 mM NaOH for the next 35 min, and the flow rate was 1 mL/min. The column temperature was set at 30 ℃ and the injection volume was 25 μL. Prior to the analyses, the samples (3 mg) were hydrolyzed by using 1 mL of 4 M trifluoroacetic acid (TFA) in an ampoule bottle at 110 °C for 8 h. The hydrolysates were dried by adding 200 μL methanol under nitrogen flow twice, diluted with deionized water to 6 mL and filtered through a 0.22 μm membrane (PES, Jiangsu Green Union Science Instrument Co., ltd, China) before injections. The monosaccharide standards including Xyl, Glc, Gal, Man, Rha, Ara, Fuc, GalA and GlcA were also derived and determined according to the same procedures as above.

Molecular weight analysis

The molecular weight of the RSPs were measured by a size-exclusion chromatogrphy (Waters Milford, MA, USA) equipped with a multi-angle laser light scattering detector (DAWN HELEOS, Wyatt Technologies Co., Santa Barbara, CA, USA) and a refractive index detector (*sEC*-MALLS-RI). Shodex SB-806 HQ and Shodex SB-804 HQ columns (7.8 × 300 mm, Shodex, Japan) was equilibrated at 25 °C and the injection volume was 50 μL. The mobile phase of distilled-deionized water containing 0.02 % NaN_3 and 0.2 M NaCl was pumped at a flow rate of 0.5 mL/min. The molecular weight of the sample was calculated using the Astra software (version 6.1.7, Wyatt Technologies Co., Santa Barbara, CA, USA) and the value of dn/dc was 0.1850 mL/g. Before analyses, the samples (3 mg) were dissolved in 1 mL of deionized water and filtered through a 0.22 μm membrane and then injected.

Scanning electron microscopy (SEM) analysis

The morphology of RSPs were evaluated by SEM (GeminiSEM 300, Zeiss, Germany). An appropriate amount of dried RSP samples were adhered to the sample stage, and coated with a layer of conductive gold film then examined under high vacuum conditions.

FT-IR spectrum analysis

The FT-IR spectrum of RSPs were obtained by Nicolet iN10 instrument (Thermo Fisher Scientific, USA). Samples were mixed evenly with KBr and pressed into tablets for FT-IR measurement in the frequency range of 4000–400 cm^{-1}.

In vitro fermentation

The RSPs fermentation *in vitro* referred to Ahmadi's method (Ahmadi et al., 2019) with some modifications. Briefly, 75 mg RSPs and Inulin were dissolved in 13.5 mL medium described as Ahmadi's method (Ahmadi et al., 2019). Fresh human feces were collected from eight healthy donors (4 males and 4 females), who had no history of gastrointestinal disease and did not take any antibiotics over 21 days. An equal amount of feces from each donor was mixed, and PBS (0.1 M, pH 7.4, v/v) was immediately added to form a suspension (10 %, w/v). After full vortex shock, the suspension was filtered with a double layer of nylon gauze. 1.5 mL filtrate was immediately added to 13.5 mL culture and incubated at 37 ℃ in the anaerobic chamber (Thermo Fisher Scientific, USA) to initiate the fermentation. 3 mL fermentation broth was taken out respectively at 0, 3, 6, 12 and 24 h and stored at −80 ℃ (U410, New Brunswick, NJ, USA) for further analysis.

Measurement of pH

The fermentation samples collected at 0, 3, 6, 12, 24 h were centrifuged at 1000 rpm for 5 min (HC-3018R, Anhui USTC Zonkia Scientific Instruments Co., ltd, China). The supernatant was transferred to a 10 mL centrifuge tube and then use the pH meter (OHAUS, Parsippany, NJ, USA) to determine the pH.

Consumption of total carbohydrates analysis

The consumption of total carbohydrates was determined based on phenol–sulfuric acid method as that of Section 2.3, which was calculated as follows:

$$\text{The consumption rate (\%)} = \frac{T_{0h} - T_{3h,6h,12hor24h}}{T_{0h}} \times 100\ \% \quad (2)$$

Scfas analysis

Before analysis, the supernatant obtained in 2.8.1 were filtered through a 0.22 μm membrane. The SCFAs were analyzed by GC-FID 6890 N (Agilent Technologies, USA) equipped with an HP-INNOWAX column (0.32 mm × 30 m, 0.25 μm, Agilent, USA) and a flame ionization detector (FID). The flow rate of nitrogen was 19 mL/min. The initial oven temperature was held at 100 °C for 0.5 min and then increased to 180 °C at a rate of 4 °C/min. The FID and injection temperature was 240 ℃ and the injection volume was 1 μL. The SCFAs content was calculated according to calibration curves of standard SCFAs (Fig. S1A).

Gut microbiota analysis

The fecal microbiota of all fermentation samples after 24 h were analyzed. Total DNA was extracted using CTBA method (Wilson, 2001). The quality of the extracted bacterial DNA was checked by 1 % (w/v) agarose gel electrophoresis. Use the specific primers 338F (5′-ACTCCTACGGGAGGCAGCAG-3′) and 806R (5′-GGACTACHVGGGTWTCTAAT-3′) to amplify the hypervariable region V3-V4 of the bacterial 16S rRNA gene. And the amplified products were sequenced on an Illumina NovaSeq platform (Novogene, Beijing, China). FIASH (v 1.2.8) was used to merge the gene sequences, and the sequences with more than 97 % similarity were classified into Operational taxonomic units (OTUs) (Zhou et al., 2020).

Statistical analysis

The data were expressed as mean ± SD (n = 3). SPSS 26.0 software (IBM Inc., Chicago, IL, USA) was used for all statistical analyses and the data were evaluated by one-way analysis of variance (ANOVA) followed by the Duncan's test while other analyses were conducted using Origin 2018 software (OriginLab Corporation, Northampton, Mass., USA). Differences were considered to be statistically significant if $p < 0.05$.

Results and discussion

Extraction yields and chemical composition

The results (Table 1) showed that different extraction methods had significant effects on the extraction yields of RSP. The yield of AK (9.26 %) was significantly higher than other methods ($p < 0.05$), demonstrating that AK could be an effective method to extract polysaccharides from *R. sterilis* S.D.Shi., which was corresponding with previous study (Sun et al., 2018). The total sugar and protein content of RSPs were listed in Table 1. The total sugar content of the four methods were

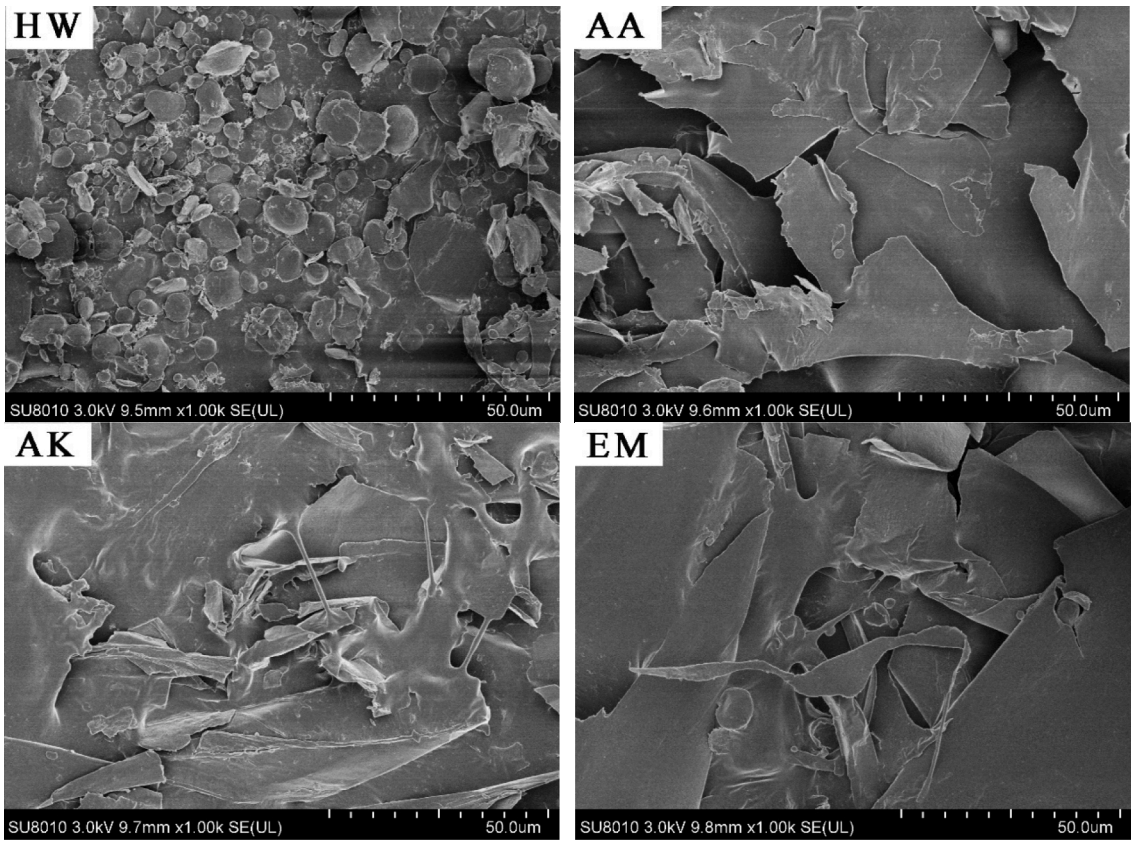

(B)

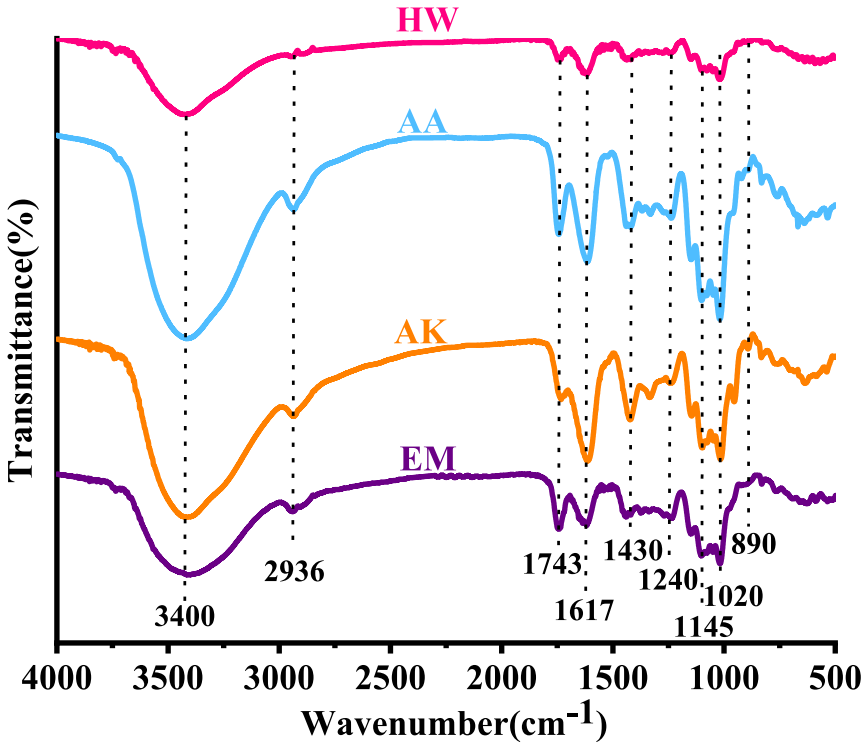

Fig. 1. (A) Scanning electron micrographs (1000×), (B) FT-IR spectrums of RSPs extracted by four different methods. RSPs: polysaccharides extracted from *R. sterilis* S.D.Shi. HW: polysaccharides extracted by hot water; AA: polysaccharides extracted by acid; AK: polysaccharides extracted by alkali, EM: polysaccharides extracted by enzyme.

Table 1
Yields and chemical composition of RSPs extracted by four different methods.

		HW	AA	AK	EM
Yield (%)		6.72 ± 0.26 b	4.12 ± 0.15 c	9.26 ± 0.63 a	4.55 ± 0.50 c
Total sugar content (%)		33.67 ± 1.64 ab	30.82 ± 1.01 b	32.94 ± 2.73 ab	36.33 ± 1.61 a
Protein content (%)		20.25 ± 1.44 a	20.50 ± 1.11 a	1.53 ± 0.91 b	22.79 ± 1.81 a
Monosaccharide composition (mol %)	Fuc	1.34 ± 0.28 b	0.91 ± 0.11 ab	1.19 ± 0.33 b	0.69 ± 0.04 a
	Rha	5.61 ± 1.03 a	5.04 ± 0.60 a	8.44 ± 0.13 b	6.20 ± 0.26 a
	Ara	7.53 ± 0.95 a	6.35 ± 0.82 a	12.05 ± 0.11 b	10.94 ± 1.08 b
	Gal	21.51 ± 1.41 b	20.52 ± 1.60 b	16.62 ± 0.96 a	26.20 ± 1.94 c
	Glc	22.55 ± 5.82 b	23.07 ± 2.37 b	6.4 ± 0.58 a	7.62 ± 2.86 a
	Man	1.43 ± 0.54 a	1.56 ± 0.72 a	1.33 ± 0.05 a	1.65 ± 0.06 a
	Xyl	2.57 ± 0.19 d	1.60 ± 0.17c	0.98 ± 0.13b	0.00 ± 0.00 a
	GalA	35.67 ± 2.08 a	39.31 ± 1.48 b	51.19 ± 0.76 d	44.54 ± 0.98 c
	GlcA	1.79 ± 0.26 a	1.64 ± 0.26 a	1.79 ± 0.04 a	2.15 ± 0.07 b
HG (%)		30.06 ± 1.26 a	34.27 ± 2.08 b	42.75 ± 0.83 d	38.35 ± 1.12 c
RG-I (%)		43.08 ± 5.81 ab	40.26 ± 4.35 a	45.56 ± 1.20 bc	49.54 ± 3.53 c
(Ara + Gal) / Rha		5.24 ± 0.52 b	5.34 ± 0.24 b	3.40 ± 0.10 a	5.99 ± 0.25 c
Linearity		0.88 ± 0.04 a	1.10 ± 0.16 b	2.24 ± 0.06 c	0.97 ± 0.09 ab
Mw (kDa)		57.55 ± 1.64 %	671.70 ± 0.33 %	922.20 ± 1.10 %	681.10 ± 0.98 %
Mn (kDa)		29.04 ± 4.23 %	98.44 ± 0.52 %	95.69 ± 4.63 %	174.8 ± 2.98 %
Mw / Mn		1.98 ± 4.55 %	6.82 ± 0.61 %	9.64 ± 4.77 %	3.90 ± 3.13 %

Data are means ± SD of three replicates. Different letters in the same row indicate significant differences among different extraction methods.
RSPs: polysaccharides extracted from *R. sterilis* S.D.Shi.
HW: polysaccharides extracted by hot water; AA: polysaccharides extracted by acid; AK: polysaccharides extracted by alkali, EM: polysaccharides extracted by enzyme.
HG (mol%) = GalA (mol%) – Rha (mol%).
RG-I (mol%) = 2Rha (mol%) + Gal (mol%) + Ara(mol%).
(Ara + Gal) / Rha: the average size of side chains.
Linearity = GalA / (Fuc + Rha + GlcA + Ara + Gal + Xyl).
Mw: weight-average molecular weight; Mn: number-average molecular weight.

respectively 36.33 % (EM), 33.67 % (HW), 32.94 % (AK), and 30.82 % (AA). Besides, there was no notable difference in the protein content (20.25 %–23.03 %) among HW-RSP, AA-RSP and EM-RSP (p greater than 0.05). While the protein content of AK-RSP was only 1.53 %, which may be attributed to the high efficiency of trypsin in removing protein (Huang et al., 2021).

The monosaccharide compositions of RSPs were shown in Table 1. The monosaccharide composition and molar percentage of RSPs obtained by different extraction methods were different. HW-RSP, AA-RSP and AK-RSP were consisted of Fuc, Rha, Ara, Gal, Glu, Man, Xyl, GalA and GlcA, while Xyl was not found in EM-RSP, probably because Xyl was easily destroyed (Wang, Yang, & Wei, 2010), which was consistent with previous study (Wang et al., 2010). Additionally, the content of Ara and Gal were significantly higher in HW-RSP and AA-RSP ($p < 0.05$), perhaps because acid and enzyme treatments caused the hydrolysis of the polysaccharide chains and also broke the intermolecular hydrogen bonds, thereby altering monosaccharide composition (Chen, Fang, Ran, Tan, Yu, & Kan, 2019). Jegou et al. (2017) also found that EM could increase the content of Gal and Ara. Besides, the Glc content in HW-RSP and AA-RSP was significantly higher ($p < 0.05$). Previous research found a novel glucan from *R. roxburghii* Tratt. (Chen and Kan, 2018), and the Glc in HW-RSP and AA-RSP was probably derived from this glucan as well. The value of RG-I (%) was calculated as 2Rha (mol%) + Gal (mol %) + Ara (mol%) (Mao et al., 2019), and the RG-I (%) value of the four RSPs were all over 40 %, indicating that RSPs were rich in Ara or Gal side chains (Zhu et al., 2020), and EM-RSP was the highest, reaching 49.54 %. The backbone of RG-I formed based on a repeating disaccharide of [→2)-α-L-Rha*p*- 1 → 4)-α-D-GalA*p*-(1 →] residues with neutral side chains attached to the O-4 position and sometimes the O-3 position of the α-L-Rha*p* backbone units. It was reported that polysaccharides with high RG-I content can exert better probiotic effects after fermentation by gut microbiota (Mao et al., 2019). The value of (Ara + Gal) / Rha in Table 1 represented the average size of side chains, and the linearity of polysaccharides was expressed by GalA / (Fuc + Rha + GlcA + Ara + Gal + Xyl) (Wang et al., 2016). There were significant differences both in linearity and the average size of side chain among the four RSPs ($p < 0.05$). AK-RSP had the highest linearity but the smallest side chain, while EM-RSP had the largest side chain. And the RG-I content, neutral sugar composition and branching degree of polysaccharides are closely related to the favorable changes of gut microbiota after polysaccharides supplementation (Mao et al., 2019). In all, these all indicated that different extraction methods obtained different structure of RSPs.

Molecular weight

The Mw and Mn of RSPs were shown in Table 1. Obviously, different extraction methods obtained different molecular weight of polysaccharides. The Mw of HW-RSP was the smallest, only 57.55 kDa, which was consistent with the result of its lowest linearity mentioned above. Wang et al. (2018) measured that the Mw of polysaccharide extracted from *R. roxburghii* Tratt. by hot water was about 6.72×10^4 Da, which was similar to this study. AK-RSP had the largest Mw of 922.20 kDa. Combined with its chemical composition, it is inferred that the main structure of AK-RSP was a long main chain with various branched chains of different sizes. AA-RSP and EM-RSP had similar Mw of 671.70 and 681.10 kDa, respectively. The value of Mw / Mn represented the polydispersity of polysaccharides (Mao et al., 2019). The polydispersity of the four RSPs were 9.64 (AK-RSP), 6.82 (AA-RSP), 3.90 (EM-RSP) and 1.98 (HW-RSP), respectively, indicating that the molecular weight distribution of AK-RSP was the widest while that of HW-RSP was the narrowest. These results indicated that different extraction methods can affect the molecular weight and size of polysaccharides, and similar results have been reported in other studies (Chen et al., 2019; Sun et al., 2018; Wang et al., 2010).

SEm

According to the SEM results of RSPs in Fig. 1A (1000×), it can be seen clearly and intuitively that the different extraction method induced different physical changes in size and shape of RSPs, which was the same as another study (Sun et al., 2018). Only the surface of HW-RSP stacked with many scattered, finely fragmented small round sheets. These fragments had a smooth surface and are mostly <10 μm in diameter. It was consistent with its lowest linearity and average molecular weight. The other three RSPs all showed a large sheet-like appearance, but their irregularity and distortion were different. The thin sections of AA-RSP and EM-RSP had more fractures, but the surface looked smoother than that of AK-RSP; AK-RSP had more folds on its surface, and most of them existed in a large aggregation except for small breakage and small fragments. These possibly due to different chemical compositions, linearity and branches (Zhao et al., 2017). Therefore, the method to extract polysaccharides needs to be taken into account, as this may be one of the determinants of the shape and structure of the polysaccharide, which in turn may affect its function.

FT-IR spectrum

FT-IR is an effective method to identify the functional groups in polysaccharides. As shown in Fig. 1B, RSPs showed similar IR signal bands of typical absorption peaks assigned to the saccharide moiety. The absorption peak at 3400 cm^{-1} represented the stretching vibration of O—H, and the peak around 2936 cm^{-1} was related to the C—H stretching vibration (Chen et al., 2019). The absorption peak at 1743 cm^{-1} was attributed to C═O stretching vibration of ester carbonyl while the absorption at 1617 cm^{-1} was assigned to the C═O stretching vibration of carboxylate ion (Wang et al., 2016). The ratio of the peak area of 1743 cm^{-1} to the sum of the two peak areas can be used to quantify the degree of esterification (Wang et al., 2016). It was evident that AK-RSP had a low degree of esterification compared to other RSPs because of the desertification under alkaline extraction conditions (Hua, Yang, Din, Chi, & Yang, 2018). The peak near 1430 cm^{-1} was attributed to the bending vibration of C—H. The peak at 1240 cm^{-1} was a characteristic of C—O—C. The absorption peaks at 1145 cm^{-1} and 1020 cm^{-1} were associated with the C—O—H side group of pyranose ring vibration and C—O—C glycosidic bond vibration, respectively (Wang et al., 2016). In addition, the characteristic absorption at 890 cm^{-1} suggested RSPs contained β -glycosidic linkages between the sugar units (Chen et al., 2019). These results indicated that different extraction methods had no clear effects on the conformation and glycosidic bond types of RSPs, which was consistent with the previous study (Chen et al., 2019; Sun et al., 2018).

Fermentation properties in vitro

Total carbohydrates and pH

The consumption of total carbohydrates and the change of pH reflected the fermentation process. Generally, gut microbiota metabolize polysaccharides to produce SCFAs that lower the pH in the gut (Huang et al., 2019). As shown in Fig. 2, the total carbohydrates consumption and pH value of the four RSPs and Inulin were significantly changed within 24 h ($p < 0.05$), but the variation trend of each RSP and Inulin was different. For total carbohydrates consumption (Fig. 2A), the total carbohydrates consumption of Inulin and the RSPs all reached more than 80 % after 24 h, indicating these could be well utilized by fecal microbiomes. However, the total carbohydrates consumption of Inulin had reached 69.50 % at 6 h, while the rapid fermentation period of the four RSPs was mainly concentrated in 6–12 h, suggesting that the fermentation rate of Inulin was faster than that of RSPs. This may be because Inulin has a small molecular weight(about 6179 Da)and can be rapidly fermented by fecal microbiomes, leading to a rapid decrease in pH (Huang et al., 2019), while RSPs have more complex structure and higher degree of substitution, which makes their fermentation speed slower. And the consumption rate of AK-RSP was relatively slow among the four RSPs, which may be due to its large molecular weight and rich content of RG-I, thereby being metabolized slowly by gut microbiota (Mao et al., 2019).

For pH, after 24 h of fermentation, the pH values of all samples decreased significantly (Fig. 2B, $p < 0.05$). The pH value of Inulin decreased fastest, but basically remained stable at about 4.50 during 12–24 h, which was similar to fermentation of Inulin in the previous study (Zhou, Zhang, Huang, Yang, & Huang, 2020). This indicated that Inulin could be considered as a fast-fermentable carbohydrate, which was consistent with the results of total carbohydrates consumption rate. The pH of AK-RSP decreased continuously and slowly, which may be related to its slow consumption rate of total carbohydrates. The pH values of HW-RSP, AA-RSP and EM-RSP increased before 12 h and then decreased. According to the results of the total carbohydrates consumption, it was speculated that the carbohydrate had been basically consumed at 12 h, and the microbiomes used the protein in the medium to produce alkaline substances such as amino acids, thus increasing the pH of fermentation broth (Sun et al., 2021). Moreover, the final pH values of AA-RSP and EM-RSP were significantly lower than HW-RSP and AK-RSP ($p < 0.05$). It was reported that low pH values were conducive to the production of a beneficial intestinal environment (Huang et al., 2019).

SCFAs

SCFAs are the main metabolites of polysaccharides fermentation by human gut microbiota, especially acetic acid, propionic acid and butyric acid (Koh et al., 2016), and more and more evidence showed that SCFAs play a positive role in the health of the host (Gentile and Weir, 2018; Huang et al., 2019; Ndeh and Gilbert, 2018). The concentrations of acetic acid, propionic acid, butyric acid, isobutyric acid, valeric acid and isovaleric acid were determined during fermentation and the results showed that there was no significant difference ($p > 0.05$) in the concentration of total SCFAs (Fig. 2C) produced by RSPs and Inulin after 24 h fermentation, but they were significantly higher than that of Blank group ($p < 0.05$), indicating that all RSPs may have similar SCFAs production capacity to Inulin. The production of SCFAs in the Blank group could be attributed to protein utilization by spoilage bacteria (Li, Pang, Yan, Shang, Hu, & Shi, 2020). Notably, the rapid increase period of total SCFAs level of AK-RSP was mainly concentrated in 12–24 h, which was consistent with the results of total carbohydrates consumption rate, suggesting that AK-RSP was a kind of slow fermentation polysaccharide, and its fermentation site might be in the distal colon. SCFAs produced in the distal colon can inhibit the metabolism of proteins and lipids that produce harmful substances, thus reducing the risk of colon cancer (Huang et al., 2019).

The main SCFA products of RSPs were acetic acid, propionic acid and butyric acid and the content of acetic acid was the most abundant, which may be related to the high content of GalA in RSPs (Mao et al., 2019). Acetic acid is also the most abundant SCFA in the peripheral circulation (Koh et al., 2016), which can cross the blood–brain barrier and reduce appetite through the central homeostatic mechanism (Huang et al., 2019). The variation trend of acetic acid concentration in each group (Fig. 2D) was similar to that of total SCFAs concentration. The acetic acid concentration of HW-RSP, AA-RSP, EM-RSP and Inulin increased rapidly in the first 12 h, but slowly in 12–24 h. However, acetic acid concentration of AK-RSP still increased significantly after 12 h ($p < 0.05$). While after 24 h, there was no significant difference in acetic acid concentration between RSPs and Inulin ($p > 0.05$). And this trend was consistent with the content of total SCFAs mentioned above.

It was reported that propionic acid can not only be converted into glucose by gluconeogenesis to induce satiety in the host (Koh et al., 2016), but also reduce the content of fatty acids in liver and plasma and inhibit the synthesis of cholesterol (Ma, Jiang, & Zeng, 2021). Overall, the concentration of propionic acid produced by the fermentation of RSPs in our results (Fig. 2E) increased by 0.37–0.80 mM, and the final concentration was higher than Inulin group. This slight increase may be caused by the fermentation of Rha and other neutral sugars in RG-I domain of RSPs (Mao et al., 2019).

As for butyric acid, it is the main energy source for colon cells, which can improve intestinal immunity and prevent intestinal inflammation and colorectal cancer (Koh et al., 2016). According to our results (Fig. 2F), the production of butyric acid was mainly concentrated at the later stage of fermentation, and the ability of RSPs to produce butyric acid was significantly higher than that of Inulin, especially AA-RSP ($p < 0.05$). The concentration of butyric acid in this group at 24 h was significantly higher than that of the other three RSPs ($p < 0.05$).

For valeric acid (Fig. S1B), isobutyric acid (Fig. S1C) and isovaleric acid (Fig. S1D), many studies have shown that they were not the main products of polysaccharide fermentation (Ding et al., 2019; Li, Xie, Huang, Shao, You, & Pedisic, 2021; Wu et al., 2021), and there was also no obvious change observed in our study.

Based on the above results, it showed that the structure of polysaccharides could affect the type, production rate and content of SCFAs during fermentation process.

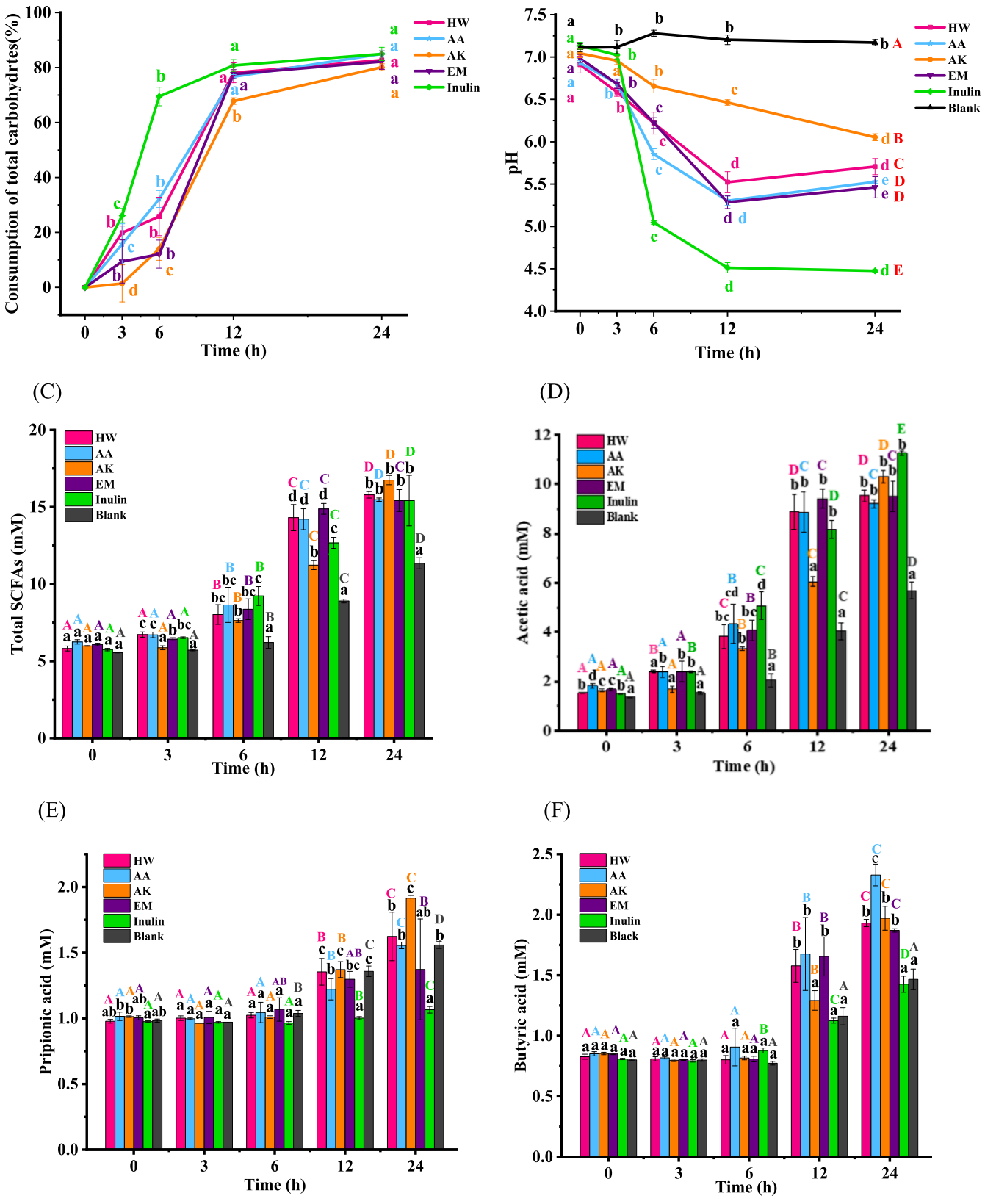

Fig. 2. (A) Total carbohydrates consumption; (B) pH value; (C) total SCFAs, (D) acetic acid, (E) propionic acid, (F) butyric acid content of RSPs during the whole fermentation process. Data are means ± SD of three replicates. Different letters of the same color represent significant differences ($p < 0.05$). RSPs: polysaccharides extracted from *R. sterilis* S.D.Shi. HW: polysaccharides extracted by hot water; AA: polysaccharides extracted by acid; AK: polysaccharides extracted by alkali, EM: polysaccharides extracted by enzyme.

Gut microbial communities

In the present study, fecal microbiota after 24 h fermentation was analyzed by 16S rRNA high throughput sequencing technology to evaluate the impact of RSPs on gut microbiota. The optimized readings were clustered into 2548 OTUs with 97 % similarity. The Venn diagram of RSPs and Inulin was shown in Fig. 3. The dot below the bar indicates the number of unique and overlapping OTUs in different group. For instance, the number of OTUs shared by the five groups was 224. The Venn diagram showed that EM-RSP had the largest number of OTU, which may be related to its highest RG-I centent (Mao et al., 2019). And previous studies have shown that the diversity of gut microbiota was negatively correlated with individual susceptibility to disease (Ma et al., 2021). Additionally, the number of OTU shared by four RSPs was only 224, indicating that the structure of RSPs had a significant effect on the diversity of gut microbiota.

The composition of gut microbiota in each group was compared at different levels. At the phylum level (Fig. 4A), Firmicutes, Bacteroidetes, Proteobacteria and Actinobacteria were the dominant bacteria among all groups, which was consistent with the results reported previously (Ma et al., 2021). However, the relative abundance of Bacteroidetes in Inulin group was obviously lower than those of RSPs, probably because the pH value of Inulin group was lower during fermentation, which was not conducive to the growth of Bacteroidetes (Li et al., 2021). Moreover, the Firmicutes / Bacteroidetes (F / B) ratio of the four RSPs were absolutely lower than that of Inulin. It was reported that lower F/B ratio was associated with lower energy intake, which might be beneficial for reducing the risk of obesity (Ma et al., 2021). Proteobacteria, including *Shigella*, *Salmonella*, *Escherichia* and other pathogenic bacteria, can affect the health of the host and cause unstable gut microbiota associated with low-grade inflammation (Zhang et al., 2020). The relative abundance of Proteobacteria of Inulin was slightly higher than RSPs. This may be due to the small molecular weight of Inulin (about 6179 Da), and Proteobacteria are most likely to use low-molecular-weight carbon sources to maintain growth (Zhang et al., 2020).

At the class level (Fig. 4B), all groups were mainly consieted of Bacterodia, Clostridia, Proteobacteria-Gammaprpteobacteria, Bacilli and Actinobacteria. Compared to the RSPs, the Inulin group had the highest abundance of Bacilli and the lowest abundance of Bacteroidia. Inulin had previously been shown to promote the growth of *Bacillus* (Zhou et al., 2020), which belongs to Bacilli and it was corresponded with our stduy. At the order level (Fig. 4C), Bacteroidales, Enterobacterales, Lachnospirales, Lactobacillales were the dominant bacteria.

At the family level (Fig. 4D), the bacteria with high relative abundance mainly included Bacteroidaccac, Enterobactcriaccac, Lachnospiraccac, Enterococcacca, Ruminococcaccac and Bifdobacteriaccac. Compared with other groups, AK-RSP had a higher relative abundance of Lachnospiraccac, and AA-RSP had a higher relative abundance of Bifidobacteriaceae. Lachnospiraccac can prevent obesity and colon cancer by producing butyric acid (Ma et al., 2021), and Bifidobacteria has many physiological functions availing to human health (Ding et al., 2019). These results indicated that RSPs significantly altered the composition of gut microbiota.

The heat map was used to compare the top 30 bacteria in different groups at the genus level, and the result was shown in Fig. 5. Generally, the relative abundance of some beneficial bacteria in RSPs, such as *Bifidobacterium*, *Lactobacillus*, *Bacteroidetes* and *Parabacteroides*, were higher than that of Inulin (Ding et al., 2019; Huang et al., 2019; Ma et al., 2021; Wu et al., 2021). To be more specfic, the relative abundance of *Bifidobacterium* in AA-RSP was the highest, but the relative abundance of *Lactobacillus* in AK-RSP and EM-RSP was higher. Both of *Bifidobacterium* and *Lactobacillus* are common probiotics (Huang et al., 2019). *Bacteroidetes* was relatively abundant in HW-RSP and was associated with SCFAs production in the gut (Li et al., 2020). Moreover, the relative abundance of *Parabacteroides* was higher in EM-RSP and *Parabacteroides* had been reported to improve metabolic disorders caused by obesity, such as hyperglycemia (Ma et al., 2021). However, some pathogenic bacteria such as *Escherichia-Shigella* was more abundant in Inulin, which may be due to its main use of carbon sources with low molecular weight

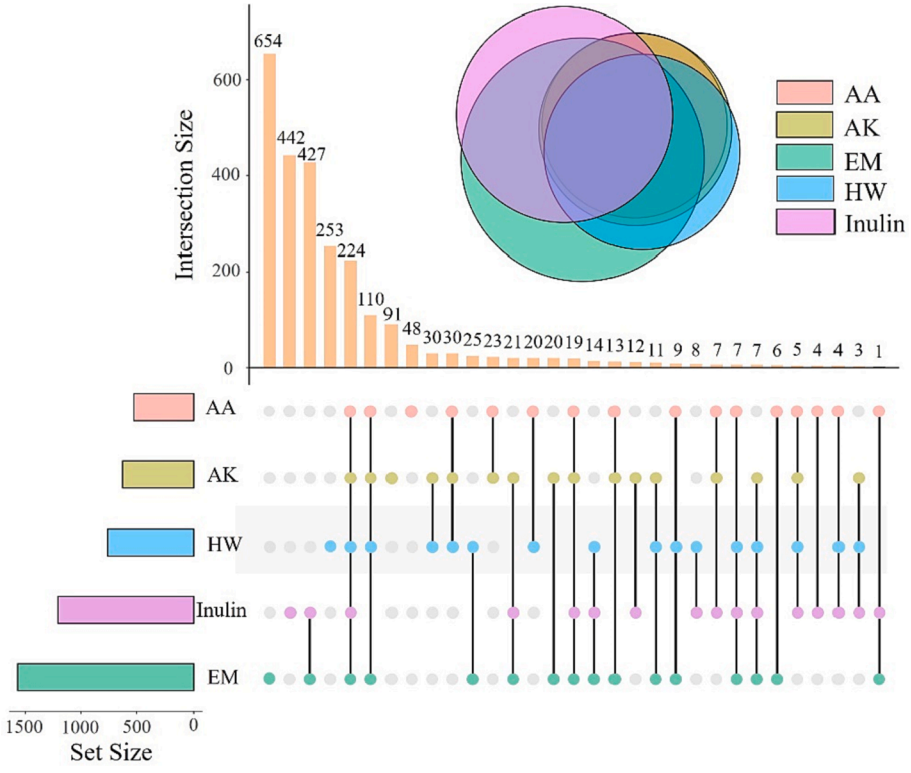

Fig. 3. Venn diagram for OTUs of RSPs. RSPs: polysaccharides extracted from *R. sterilis* S.D.Shi. HW: polysaccharides extracted by hot water; AA: polysaccharides extracted by acid; AK: polysaccharides extracted by alkali, EM: polysaccharides extracted by enzyme.

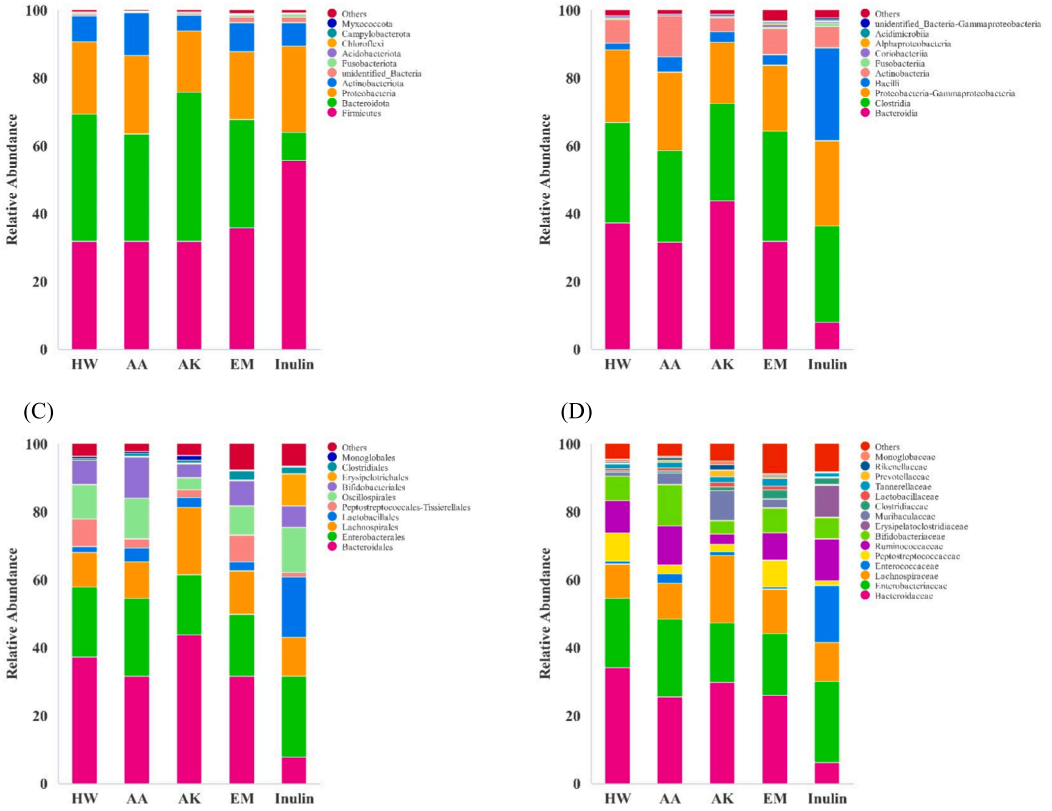

Fig. 4. Comparison of gut microbiota of RSPs and Inulin. (A) the relative abundance of gut microbiota at phylum level, (B) the relative abundance of gut microbiota at class level, (C) the relative abundance of gut microbiota at order level, (D) the relative abundance of gut microbiota at family level. RSPs: polysaccharides extracted from *R. sterilis* S.D.Shi. HW: polysaccharides extracted by hot water; AA: polysaccharides extracted by acid; AK: polysaccharides extracted by alkali, EM: polysaccharides extracted by enzyme.

to maintain its growth (Wu et al., 2021). And it was reported that *Escherichia-Shigella* may cause gut microbiota imbalance, resulting in intestinal inflammation (Zhang et al., 2020). Besides, *Enterococcus* and *Erysipelotrichaceae-UCG-003* also had a higher abundance in Inulin.

T-test was used to compare the bacteria of each RSP and Inulin, respectively, to further verify the difference between their gut microbiota, and the results (Fig. S2) were consistent with the above analysis. *Bacteroidetes, Escherichia-Shigella,Enterococcus* and *Erysipelotrichaceae-UCG-003* etc. all showed significant differences between RSPs and Inulin ($p < 0.05$). And the relative abundance of Bifidobacterium in AA-RSP was significantly higher than that in Inulin ($p < 0.01$). These results suggested that RSPs can regulate the composition of gut microbiota and promote the proliferation of beneficial bacteria. Moreover, the probiotic effects of RSPs with different structures were different.

In order to specifically compare the taxa differences among RSPs with different structures, LEfSe analysis (Fig. S3) was performed. According to the LDA scores (log10, >3), a total of 60 bacterial taxa were markedly enriched in different groups, including 24 taxa in Inulin (purple), 9 taxa in HW-RSP (orange), 7 taxa in AA-RSP (red), 11 taxa in AK-RSP (green) and 9 taxa in EM-RSP (blue). For instance, HW-RSP mianly promoted the growth of Bacteroidaceae family, *Bacteroides* and its next-generations, such as *Bacteroides_vulgatus* and *Bacteroides_uniformis*. While AA-RSP visibly promoted the growth of Bifidobacteriaceae family and its generations. AK-RSP significantly increased the abundance of Bacteroidales and Monoglobales. As for EM-RSP, it mainly showed obvious increase in the abundance of Gemmationadetes.

In order to more clearly evaluate the impact of RSPs structure on gut microbiota, Spearman was used to analyze the correlation among the structure of RSPs, SCFA production level and the top 5 bacteria in abundance at genus level. Results were presented in Fig. S4.

Bacteroides showed significant positive correlation (r = 0.75) with propionic acid production, which was consistent with other research results (Li et al., 2020). In addition, *Bifidobacterium* were also correlated with butyric acid. In the previous LEfSe analysis, it was found that AA-RSP significantly promoted the growth of *Bifidobacterium*, which precisely explained the highest concentration of butyric acid generated in the AA-RSP. But other studies showed that *Bifidobacterium* was mainly associated with the production of acetic acid (Koh et al., 2016; Wu et al., 2021), which may be caused by the differences between the people who providing faeces (Wu et al., 2017). It was reported that *Faecalibacterium* can consume acetic acid to produce butyric acid and anti-inflammatory factors (Ma et al., 2021), and it also showed a negative correlation with acetic acid (r = -0.59) in our study. Previous study reported that acetic acid was produced mainly by the fermentation of Gal and GalA, the production of propionic acid was due to the fermentation of Ara and Glc, and the production of butyric acid was attributed to GalA (Wang et al., 2019). But in our study, both Rha and Ara showed a strong positive correlation with acetic acid (r = 0.73, 0.75) and propionic acid (r = 0.79, 0.82), which might be caused by the difference of raw materials, fecal microbiota and culture medium (Song et al., 2021; Wu et al., 2017).

Besides, the composition and structure of polysaccharides also had obvious correlation with bacterial community. Similar to the results reported, favorable changes in the composition of bacteria were closely related to neutral sugars and the degree of side chain (Mao et al., 2019). To be more specific, *Bacterides* showed positive correlation with Ara, because 60 % of *Bacteroides* could degrade arabinoglycan side chain in RG- I region (Mao et al., 2019). *Escherichia-shigella*, *Bifidobacterium*, *Faecalibacterium* and *Paraclostrium* were all positively correlated with Gal, and the top three bacteria were also positively related to Glc. It can be found that *Bifidobacterium* had a strong connection with Glc. Previous study has compared the molar growth yield of *Bifidobacterium S 324* on different monosaccharides, the results showed that except Lac, its molar

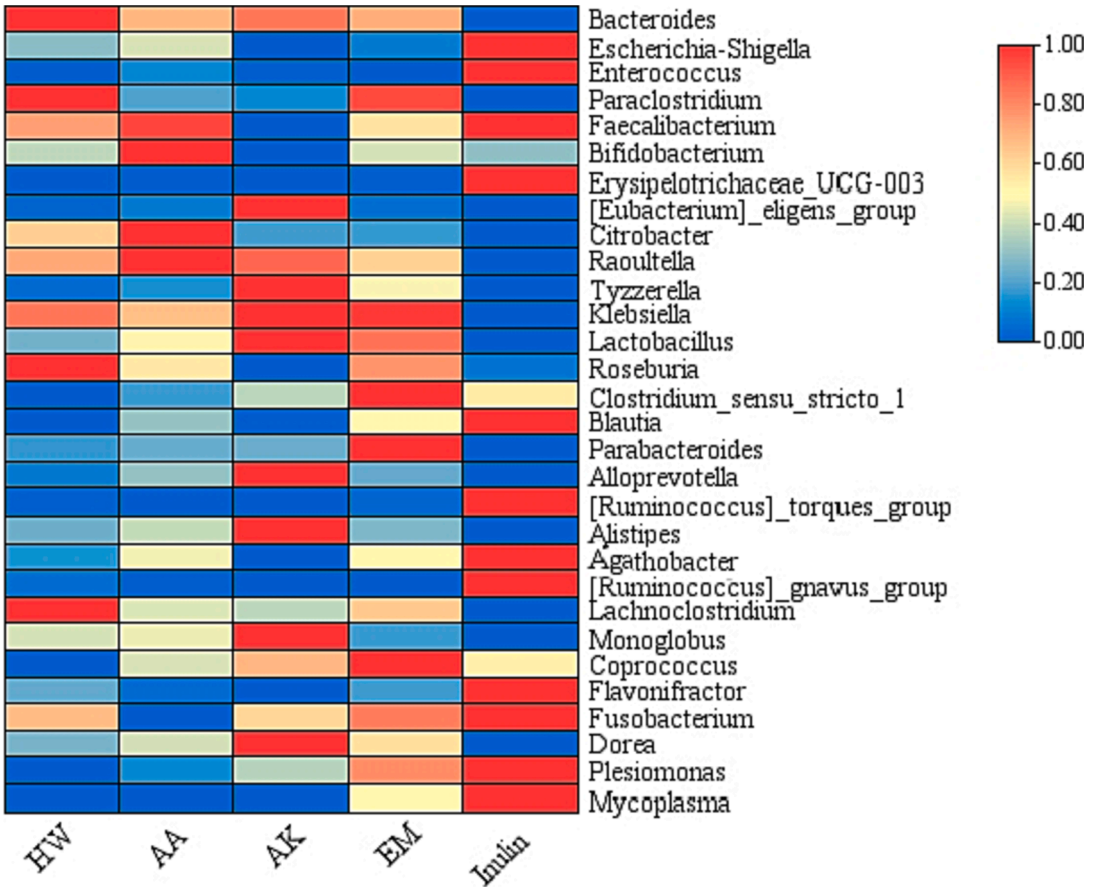

Fig. 5. Heat map of gut microbiota of RSPs and Inulin based on the relative abundance of the top 30 genera at genus level. RSPs: polysaccharides extracted from *R. sterilis* S.D.Shi. HW: polysaccharides extracted by hot water; AA: polysaccharides extracted by acid; AK: polysaccharides extracted by alkali, EM: polysaccharides extracted by enzyme.

growth yield in Glc was the highest (de Vries & Stouthamer, 1968), confirming the results of this study. Furthermore, the overall top 5 bacteria were negatively correlated with the linearity of polysaccharides, while the side chain size was positively associated with them. This indicated that polysaccharides with high branching degree can promote the growth of bacteria, especially beneficial bacteria (Zhu et al., 2020). Moreover, according to the results of this study, *Bifidobacterium* and *Faecalibacterium* may be synergistic and mutually promoting.

As shown in Fig. S5, PICRUST was used to analyze the associated KEGG pathways in order to predict the metabolic function of gut microbiota. The metabolic pathways of RSPs and Inulin showed extremely high similarity, including membrane transport, carbohydrate metabolism, amino acid metabolism, replication and repair, energy metabolism, etc., but their abundance were different. Compared to Inulin, the metabolic pathways of HW-RSP, AA-RSP and AK-RSP were mostly attenuated, while 35 metabolic pathways were enhanced in EM-RSP.

To further evaluate the effects of RSPs on the metabolism of polysaccharides, lipids and proteins in gut microbiota, iPath was used to analyze the specific metabolic pathways of RSPs (Fig. S6). In the figure, pink represented the common metabolic pathway of RSP and Inulin, green represented the unique metabolic pathway of Inulin, and other colors represented the unique metabolic pathway of corresponding RSP.

Compared with Inulin, HW-RSP (Fig. S6A) had special metabolic pathways in lipid metabolism and biosynthesis of other secondary metabolites. They included glycerophospholipid metabolism, sphingolipid metabolism, steroid biosynthesis, primiary bile acid biosynthesis and indole alkaloid biosynthesis. AA-RSP (Fig. S6B) and AK-RSP (Fig. S6C) had the same specific metabolic pathway, namely peptidogilycan biosynthesis and lysine biosynthesis. Surprisingly, EM-RSP (Fig. S6D) not only contained almost all of the characteristic metabolic pathways of the other three RSPs mentioned above, and it also contained archidonic acid metabolism, xylene degradation, penicillin and cephalosporin biosynthesis, caffeine metabolism and amino acid metabolism including lysine, serine, threonine, arginine and proline. Previous results showed that EM-RSP had the highest number of OTU and the highest diversity of microbiota, which may explained why it had the most unique metabolic pathways. These results suggest that RSPs can regulate the metabolism of gut microbiota, improve intestinal health as Inulin and have the possibility to become a potential prebiotics.

Conclusion

In this study, the effects of four different extraction methods on the yield, structure and *in vitro* fermentation characterizations of RSPs were compared. HW-RSP and AA-RSP showed high content of Gal, Glc and GalA. The molecular weight of HW-RSP was the smallest, and it was fragmentary under SEM. AK-RSP had the highest GalA content and the largest molecular weight. And EM-RSP were rich in RG-I and showed the highest degree of branched chain. All RSPs promoted the production of SCFAs, mainly acetic acid, propionic acid and butyric acid. And RSPs regulated the composition of gut microbiota by promoting the growth of beneficial bacteria like *Bifidobacterium*, *Bacteroides, Faecalibacterium* and *Paraclostrium* to varying degrees, but inhibiting the growth of harmful bacteria such as *Escherichia-shigella*. Among four RSPs, EM-RSP exhibited the best microbial diversity and the function prediction results showed that EM-RSP had the most special metabolic pathways. All these

results suggested that RSPs had good probiotics potential, and could be developed as functional foods. At the same time, the research of potential functions of *R. sterilis* S.D.Shi polysaccharides is of great significance to improve the development and utilization of *R. sterilis* S.D.Shi resources and expand its development prospects. The limitation here is that only *in vitro* simulated fermentation was performed, further *in vivo* experiments would be employed to confirm these conclusions.

Declaration of Competing Interest

The authors declare that they have no known competing financial interests or personal relationships that could have appeared to influence the work reported in this paper.

Data availability

Data will be made available on request.

Acknowledgments

This work was supported by the project of Youth Program of the National Natural Science Foundation of China (32202071), Zhejiang Basic Public Welfare Research Project (LQ22C200003), China Postdoctoral Science Foundation (2021M692832), the priority funding of Zhejiang province (2021C02001), the Fundamental Research Funds for the Central Universities (2021FZZX001-54) and the Independent preresearch project of Innovation Center of Yangtze River Delta (2022ZY001).

Appendix A. Supplementary data

Supplementary data to this article can be found online at https://doi.org/10.1016/j.fochx.2022.100533.

References

Ahmadi, S., Wang, S., Nagpal, R., Mainali, R., Soleimanian-Zad, S., Kitzman, D., & Yadav, H. (2019). An *in vitro* batch-culture model to estimate the effects of interventional regimens on human fecal microbiota. *Journal of Visualized Experments, 149*. https://doi.org/10.3791/59524

Bradford, M. M. (1976). Rapid and sensitive method for quantitation of microgram quantities of protein utilizing principle of protein-dye binding. *Analytical Biochemistry, 72*(1–2), 248–254. https://doi.org/10.1006/abio.1976.9999

Chen, G., Fang, C., Ran, C., Tan, Y., Yu, Q., & Kan, J. (2019). Comparison of different extraction methods for polysaccharides from bamboo shoots (Chimonobambusa quadrangularis) processing by-products. *International Journal of Biological Macromolecules, 130*, 903–914. https://doi.org/10.1016/j.ijbiomac.2019.03.038

Chen, G., & Kan, J. (2018). Characterization of a novel polysaccharide isolated from *Rosa roxburghii* Tratt fruit and assessment of its antioxidant *in vitro* and *in vivo*. *International Journal of Biological Macromolecules, 107*(Pt A), 166–174. https://doi.org/10.1016/j.ijbiomac.2017.08.160

de Vries, W., & Stouthamer, A. (1968). Fermentation of glucose, lactose, galactose, mannitol, and xylose by bifidobacteria. *Journal of Bacteriology, 96*(2), 472–478.

Ding, Y., Yan, Y., Peng, Y., Chen, D., Mi, J., Lu, L., … Cao, Y. (2019). In vitro digestion under simulated saliva, gastric and small intestinal conditions and fermentation by human gut microbiota of polysaccharides from the fruits of Lycium barbarum. *International Journal of Biological Macromolecules, 125*, 751–760. https://doi.org/10.1016/j.ijbiomac.2018.12.081

Dubois, M., Gilles, K., Hamilton, J. K., Rebers, P. A., & Smith, F. (1951). A colorimetric method for the determination of sugars. *Nature, 168*(4265), 167. https://doi.org/10.1038/168167a0

Gentile, C. L., & Weir, T. L. (2018). The gut microbiota at the intersection of diet and human health. *Science, 362*(6416), 776–780. https://doi.org/10.1126/science.aau5812

Hou, Z., Hu, X., Luan, L., Yu, C., Wang, X., Chen, S., & Ye, X. (2022). Prebiotic potential of RG-I pectic polysaccharides from Citrus subcompressa by novel extraction methods. *Food Hydrocolloids, 124*. https://doi.org/10.1016/j.foodhyd.2021.107213

Hou, Z., Yang, H., Zhao, Y., Xu, L., Zhao, L., Wang, Y., & Liao, X. (2020). Chemical characterization and comparison of two chestnut rose cultivars from different regions. *Food Chemistry, 323*, Article 126806. https://doi.org/10.1016/j.foodchem.2020.126806

Hua, X., Yang, H., Din, P., Chi, K., & Yang, R. (2018). Rheological properties of deesterified pectin with different methoxylation degree. *Food Bioscience, 23*, 91–99. https://doi.org/10.1016/j.fbio.2018.03.011

Huang, G., Chen, F., Yang, W., & Huang, H. (2021). Preparation, deproteinization and comparison of bioactive polysaccharides. *Trends in Food Science & Technology, 109*, 564–568. https://doi.org/10.1016/j.tifs.2021.01.038

Huang, J., Wang, Q., Xu, Q., Zhang, Y., Lin, B., Guan, X., … Zheng, Y. (2019). *In vitro* fermentation of Oacetylarabinoxylan from bamboo shavings by human colonic microbiota. *International Journal of Biological Macromolecules, 125*, 27–34. https://doi.org/10.1016/j.ijbiomac.2018.12.024

Jegou, S., Hoang, D. A., Salmon, T., Williams, P., Oluwa, S., Vrigneau, C., … Marchal, R. (2017). Effect of grape juice press fractioning on polysaccharide and oligosaccharide compositions of Pinot meunier and Chardonnay Champagne base wines. *Food Chemistry, 232*, 49–59. https://doi.org/10.1016/j.foodchem.2017.03.032

Koh, A., De Vadder, F., Kovatcheva-Datchary, P., & Backhed, F. (2016). From dietary fiber to host physiology: Short-chain fatty acids as key bacterial metabolites. *Cell, 165*(6), 1332–1345. https://doi.org/10.1016/j.cell.2016.05.041

Li, J., Pang, B., Yan, X., Shang, X., Hu, X., & Shi, J. (2020). Prebiotic properties of different polysaccharide fractions from Artemisia sphaerocephala Krasch seeds evaluated by simulated digestion and in vitro fermentation by human fecal microbiota. *International Journal of Biological Macromolecules, 162*, 414–424. https://doi.org/10.1016/j.ijbiomac.2020.06.174

Li, X., Xie, Q., Huang, S., Shao, P., You, L., & Pedisic, S. (2021). Digestion & fermentation characteristics of sulfated polysaccharides from Gracilaria chouae using two extraction methods in *vitro* and *in vivo*. *Food Research International, 145*, Article 110406. https://doi.org/10.1016/j.foodres.2021.110406

Liu, M. H., Zhang, Q., Zhang, Y. H., Lu, X. Y., Fu, W. M., & He, J. Y. (2016). Chemical analysis of dietary constituents in *Rosa roxburghii* and *Rosa sterilis* fruits. *Molecules, 21*(9). https://doi.org/10.3390/molecules21091204

Ma, Y., Jiang, S., & Zeng, M. (2021). In vitro simulated digestion and fermentation characteristics of polysaccharide from oyster (Crassostrea gigas), and its effects on the gut microbiota. *Food Research International, 149*, Article 110646. https://doi.org/10.1016/j.foodres.2021.110646

Mao, G., Li, S., Orfila, C., Shen, X., Zhou, S., Linhardt, R. J., … Chen, S. (2019). Depolymerized RG-I-enriched pectin from citrus segment membranes modulates gut microbiota, increases SCFA production, and promotes the growth of Bifidobacterium spp., Lactobacillus spp. and Faecalibaculum spp. *Food Function, 10*(12), 7828–7843. https://doi.org/10.1039/c9fo01534e

Ndeh, D., & Gilbert, H. J. (2018). Biochemistry of complex glycan depolymerisation by the human gut microbiota. *FEMS Microbiology Reviews, 42*(2), 146–164. https://doi.org/10.1093/femsre/fuy002

Song, Q., Wang, Y., Huang, L., Shen, M., Yu, Y., Yu, Q., … Xie, J. (2021). Review of the relationships among polysaccharides, gut microbiota, and human health. *Food Research International, 140*, Article 109858. https://doi.org/10.1016/j.foodres.2020.109858

Sun, Y., Hou, S., Song, S., Zhang, B., Ai, C., Chen, X., & Liu, N. (2018). Impact of acidic, water and alkaline extraction on structural features, antioxidant activities of Laminaria japonica polysaccharides. *International Journal of Biological Macromolecules, 112*, 985–995. https://doi.org/10.1016/j.ijbiomac.2018.02.066

Sun, Y., Hu, J., Zhang, S., He, H., Nie, Q., Zhang, Y., … Nie, S. (2021). Prebiotic characteristics of arabinogalactans during *in vitro* fermentation through multi-omics analysis. *Food and Chemical Toxicology, 156*, Article 112522. https://doi.org/10.1016/j.fct.2021.112522

Wang, H., Li, Y., Ren, Z., Cong, Z., Chen, M., Shi, L., … Pei, J. (2018). Optimization of the microwave-assisted enzymatic extraction of Rosa roxburghii Tratt. polysaccharides using response surface methodology and its antioxidant and α-D-glucosidase inhibitory activity. *International Journal of Biological Macromolecules, 112*, 473–482. https://doi.org/10.1016/j.ijbiomac.2018.02.003

Wang, L., Chen, C., Zhang, B., Huang, Q., Fu, X., & Li, C. (2018). Structural characterization of a novel acidic polysaccharide from *Rosa roxburghii* Tratt fruit and its α-glucosidase inhibitory activity. *Food Function, 9*(7), 3974–3985. https://doi.org/10.1039/c8fo00561c

Wang, L., Li, C., Huang, Q., Fu, X., & Liu, R. H. (2019). In vitro digestibility and prebiotic potential of a novel polysaccharide from *Rosa roxburghii* Tratt fruit. *Journal of Functional Foods, 52*, 408–417. https://doi.org/10.1016/j.jff.2018.11.021

Wang, W., Ma, X., Jiang, P., Hu, L., Zhi, Z., Chen, J., … Liu, D. (2016). Characterization of pectin from grapefruit peel: A comparison of ultrasound-assisted and conventional heating extractions. *Food Hydrocolloids, 61*, 730–739. https://doi.org/10.1016/j.foodhyd.2016.06.019

Wang, Y., Yang, Z., & Wei, X. (2010). Sugar compositions, alpha-glucosidase inhibitory and amylase inhibitory activities of polysaccharides from leaves and flowers of Camellia sinensis obtained by different extraction methods. *International Journal of Biological Macromolecules, 47*(4), 534–539. https://doi.org/10.1016/j.ijbiomac.2010.07.007

Wilson, K. (2001). Preparation of genomic DNA from bacteria. *Current protocols in molecular biology, Chapter 2*, Unit 2.4-Unit 2.4. https://doi.org/10.1002/0471142727.mb0204s56.

Wu, D. T., Yuan, Q., Guo, H., Fu, Y., Li, F., Wang, S. P., & Gan, R. Y. (2021). Dynamic changes of structural characteristics of snow chrysanthemum polysaccharides during *in vitro* digestion and fecal fermentation and related impacts on gut microbiota. *Food Research International, 141*, Article 109888. https://doi.org/10.1016/j.foodres.2020.109888

Wu, Q., Pi, X., Liu, W., Chen, H., Yin, Y., Yu, H. D., … Zhu, L. (2017). Fermentation properties of isomaltooligosaccharides are affected by human fecal enterotypes. *Anaerobe, 48*, 206–214. https://doi.org/10.1016/j.anaerobe.2017.08.016

Xu, J., Vidyarthi, S. K., Bai, W., & Pan, Z. (2019). Nutritional constituents, health benefits and processing of *Rosa Roxburghii*: A review. *Journal of Functional Foods, 60*. https://doi.org/10.1016/j.jff.2019.103456

Zhang, X., Aweya, J. J., Huang, Z., Kang, Z., Bai, Z., Li, K., … Cheong, K. L. (2020). In vitro fermentation of Gracilaria lemaneiformis sulfated polysaccharides and its agaro-oligosaccharides by human fecal inocula and its impact on microbiota. *Carbohydrate Polymer, 234*, Article 115894. https://doi.org/10.1016/j.carbpol.2020.115894

Zhao, C., Li, X., Miao, J., Jing, S., Li, X., Huang, L., & Gao, W. (2017). The effect of different extraction techniques on property and bioactivity of polysaccharides from Dioscorea hemsleyi. *International Journal of Biological Macromolecules, 102*, 847–856. https://doi.org/10.1016/j.ijbiomac.2017.04.031

Zhou, L., Li, H., Qin, J. G., Wang, X., Chen, L., Xu, C., & Li, E. (2020). Dietary prebiotic inulin benefits on growth performance, antioxidant capacity, immune response and intestinal microbiota in Pacific white shrimp (Litopenaeus vannamei) at low salinity. *Aquaculture, 518*. https://doi.org/10.1016/j.aquaculture.2019.734847

Zhou, X., Zhang, Z., Huang, F., Yang, C., & Huang, Q. (2020). *In vitro* digestion and fermentation by human fecal microbiota of polysaccharides from flaxseed. *Molecules, 25*(19). https://doi.org/10.3390/molecules25194354

Zhu, K., Mao, G., Wu, D., Yu, C., Cheng, H., Xiao, H., Ye, X., Linhardt, R. J., & Chen, S. (2020). Highly branched RG-I domain enrichment is indispensable for pectin mitigating against high-fat diet-induced obesity. *Journal of Agricultural and Food Chemistry, 68*(32), 8688–8701. https://doi.org/10.1021/acs.jafc.0c02654